ELSEVIER

Biophysical Chemistry 101–102 (2002) 211–219

Biophysical Chemistry

www.elsevier.com/locate/bpc

Charge–charge interactions are the primary determinants of the p*K* values of the ionizable groups in Ribonuclease T1☆

C. Nick Pace[a,*], Beatrice M.P. Huyghues-Despointes[a], James M. Briggs[b], Gerald R. Grimsley[a], J. Martin Scholtz[a,*]

[a]*Department of Medical Biochemistry and Genetics, Department of Biochemistry and Biophysics, and Center for Advanced Biomolecular Research, Texas A&M University, College Station, TX 77843-1114, USA*
[b]*Department of Biology and Biochemistry, University of Houston, Houston, TX 77204-5001, USA*

Received 11 January 2002; received in revised form 14 February 2002; accepted 14 February 2002

Abstract

Coulomb's law and a finite difference Poisson–Boltzmann based analysis are used to predict the p*K* values for 15 ionizable side chains (6 Asp, 6 Glu and 3 His) in ribonuclease T1. These predicted values are compared to the measured p*K* values to gain insight into the most important factors that influence the p*K* values of the ionizable groups in proteins. Charge–charge interactions are clearly the most important factor that determines the p*K* values of most ionizable groups in ribonuclease T1. However, p*K* values can be shifted by several p*K* units by the Born self energy associated with burying ionizable groups and by favorable intramolecular hydrogen bonding.

Keywords: p*K*; Coulomb's law; Finite difference Poisson–Boltzmann equation; Born self energy; Hydrogen bonds; Charge–charge interactions

1. Introduction

Spitzner et al. [1] used two-dimensional heteronuclear NMR spectroscopy to measure the p*K* values of the 6 Asp, 6 Glu and 3 His side chains in ribonuclease T1 (RNase T1). In two succeeding papers, Koumanov et al. [2,3] used a finite difference Poisson–Boltzmann analysis to predict the p*K* values for the same residues. In some cases, the predicted values differ markedly from the measured values. We have predicted the same p*K* values using Coulomb's law and a finite difference Poisson–Boltzmann based approach using the University of Houston Brownian dynamics package (UHBD), another widely used method [4–6]. By comparing the results of these analyses, we are able to gain insight into the key factors that determine the p*K* values of the ionizable groups in RNase T1. Several other groups have considered this same question [6–16].

☆ We are delighted to dedicate this paper to Dr John Schellman, a scientist for all seasons.

*Corresponding authors. Tel.: +1-979-845-1788 (CNP); +1-979-845-0828 (JMS); fax: +1-979-847-9481.
E-mail address: nickpace@tamu.edu (C.N. Pace), jmscholtz@tamu.edu (J.M. Scholtz).

0301-4622/02/$ - see front matter
PII: S0301-4622(02)00192-8

Table 1
Measured and calculated pK values of 15 ionizable side chains in RNase T1

Residue	pK (measured)[a]	pK (CL)[b]	pK (UHBD)[b]	pK (combined)[b]
Asp(4.0)[c]				
3	3.51	3.66	3.67	3.41
15	3.49	3.72	3.64	3.35
29	4.44	3.57	4.11	4.00
49	4.37	4.22	4.21	4.30
66	3.89	3.92	3.92	3.86
76	0.5	2.69	2.56	2.13
Glu(4.4)[c]				
28	5.39	4.52	4.82	4.86
31	4.78	4.55	4.82	4.91
46	3.58	3.88	4.88	4.28
58	3.93	3.22	2.52	3.58
82	3.24	3.07	2.99	2.90
102	5.16	5.32	5.02	5.28
His(6.3)[c]				
27	7.08	7.78	7.59	7.65
40	7.75	7.75	7.12	7.72
92	7.31	7.53	7.08	7.56
RMSD[d]		0.72 (0.45)	0.78 (0.60)	0.54 (0.35)

[a] Except for Asp 76, the pK values were measured at 35 °C as described by Spitzner et al. [1] and given in Koumanov et al. [2]. The pK for Asp 76 was measured at 25 °C as described by Giletto and Pace [33].

[b] pK (CL) was calculated using Coulomb's law as described in the text. pK (UHBD) was calculated by a finite difference Poisson–Boltzmann based approach using the University of Houston Brownian dynamics package (UHBD). UHBD is described in [4–6]. pK (combined) was calculated using the charge–charge interaction term from Coulomb's law, ΔG_{ij}(CL), and the charge–partial charge interaction term, ΔG(BG), and the Born term, ΔG(Born), from UHBD. In all cases, the coordinates are from the PDB structure 9RNT [18] and single charges were placed on the following atoms: Cγ for Asp; Cδ for Glu; Cε1 for His; Nζ for Lys; and Cζ for Arg.

[c] These are the pK values expected for these side chains in uncharged peptides [17].

[d] The first RMSD includes the results for Asp 76, and the term in parentheses does not.

2. Results

The measured pK values for RNase T1 are given in Table 1 [1,2]. The pK values, calculated by three different methods, are also given in Table 1. The methods used to calculate the pK values are described next.

In addition to the 15 measured pK values, RNase T1 contains 14 other ionizable groups (the N- and C-termini, 9 Tyr, 2 Lys and 1 Arg residues). We assumed the following pK values based on model compounds from Nozaki and Tanford [17]for these residues: α-COOH (3.8), α-NH_3^+ (7.5), Tyr (9.6), Lys (10.4) and Arg (12.0). We assume that the Tyr, Lys and Arg residues will not ionize in the pH range we are considering, $<$pH 9, for the 15 ionizable groups in Table 1. We use Coulomb's law (CL):

$$\Delta G_{ij}(\mathrm{CL}) = \sum_j q_i q_j / \varepsilon r \quad (1)$$

to sum up the charge–charge interactions at a pH equal to the pK of each ionizing group being considered and the rest of the charges on the protein. Since we are at the pK, we use a charge of -0.5 for the Asp or Glu residues under consideration and a charge of $+0.5$ for the pK calculation for the His residues. For the other residues, their measured pK is used to calculate their net charge at the pH being considered. The distance r between the two charges is calculated using the 1.5 Å resolution crystal structure of RNase T1 determined by Martinez-Oyanedel et al. [18] (Table 1). (Pfeiffer et al. [19] have carefully compared this crystal structure with the solution structure deter-

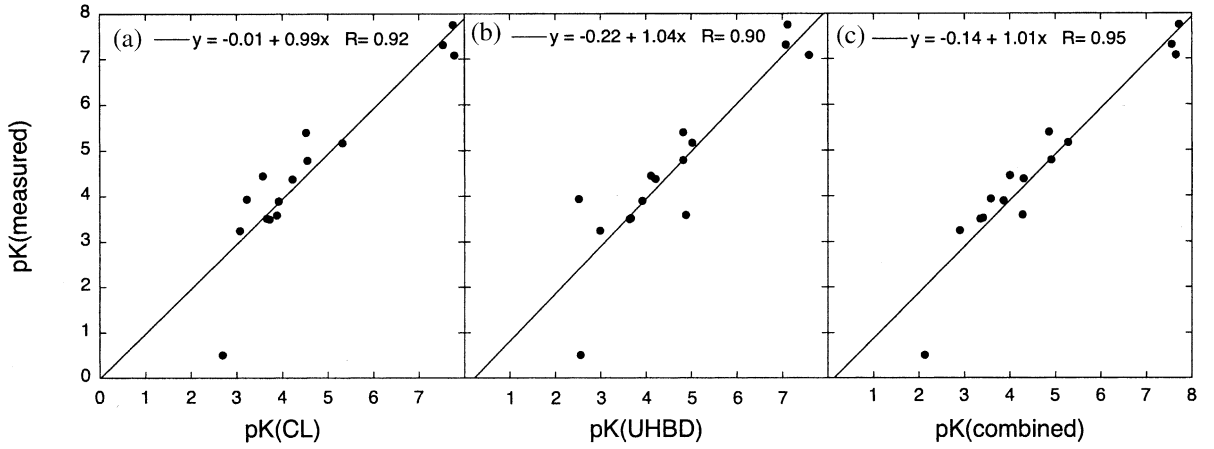

Fig. 1. Shown are correlation plots between the measured and calculated p*K* values of RNase T1 using Coulomb's law (a), UHBD (b) and a combination of both methods (c). If the data point for Asp 76 is removed, the *R*-values become 0.96 (a), 0.92 (b) and 0.98 (c).

mined by NMR.) For reasons explained below, a dielectric constant, $\varepsilon = 45$, was chosen for all of the calculations. Fig. 1 shows plots of the p*K* (measured) values vs. the p*K* (calculated) values. Note that using $\varepsilon = 45$ leads to slopes near one for all three of the plots.

The p*K* (UHBD) values were calculated by a finite difference Poisson–Boltzmann based approach using the University of Houston Brownian Dynamics package (UHBD) [4–6] with the following adjustable parameters: $\varepsilon_{protein} = 45$; $\varepsilon_{solvent} = 75$; T = 35 °C; ionic strength = 20 mM; Stern Layer = 2.0 Å; CHARMM 19 charge parameter set; [20]; and probe radius = 1.4 Å. The $\varepsilon_{protein} = 45$ value was chosen because it gave the lowest root mean square deviation (RMSD) between the p*K* (measured) and p*K* (UHBD) values. Most often, a value of $\varepsilon_{protein} = 20$ is used with this program [6,16]. With $\varepsilon_{protein} = 20$, the RMSD = 0.89, which is considerably worse than the RMSD = 0.78 when $\varepsilon_{protein} = 45$ is used (Table 1).

The p*K* (CL) calculation takes into account only charge–charge interactions between the ionizable group and the other charged groups on the protein which we designate ΔG_{ij}(CL). The UHBD program takes into account three terms:

$$\Delta G_i = \Delta G_{ij}(\mathrm{UHBD}) + \Delta G(\mathrm{BG}) + \Delta G(\mathrm{Born}) \quad (2)$$

where ΔG_{ij}(UHBD) is the charge–charge interaction term, ΔG(BG) is a summation of the interaction of the ionizable group with the partial charges of the polar groups in the protein and ΔG(Born) is the Born self energy of transferring a charge from the solvent to the protein. The CL calculation might be expected to model ΔG_{ij} better than UHBD because the actual p*K* values of the ionizable groups are used in the calculation. In UHBD, the calculated p*K* values are used to calculate the net charges. To test this, we combined the ΔG_{ij} term from the CL calculation with the ΔG(BG) and ΔG(Born) terms from UHBD calculation and this is denoted ΔG(combined) in Table 1. Note that the RMSD is considerably lower for the p*K* (combined) values than for the p*K* (CL) or p*K* (UHBD) values.

3. Discussion

For all of the p*K* calculations, we begin with the p*K* of the ionizable group in an uncharged peptide. We have used the values from Nozaki and Tanford [17] that are most often used in trying to understand what determines the p*K* values of ionizable groups in folded proteins [6,7,11,21]. In Table 2, we give the difference between the measured p*K* values and the uncharged peptide p*K* values. Some of the p*K* values of the carboxyl

Table 2
Factors influencing the pK values for 15 ionizable side chains in RNase T1

Residue	ΔpK[a]	ΔG[b] (kcal/mol)	ΔG_{ij}(CL)[c] (kcal/mol)	ΔG_{ij}(UHBD)[d] (kcal/mol)	Buried[e] (%)	ΔG(Born)[f] (kcal/mol)	HB[g] (#)	ΔG(BG)[h] (kcal/mol)
Asp								
3	−0.49	0.69	0.48	0.83	38	0.17	1	−0.53
15	−0.51	0.72	0.39	1.03	58	0.24	1	−0.76
29	0.44	−0.62	0.60	−0.76	51	0.16	0	0.44
49	0.37	−0.52	−0.31	−0.41	8	0.05	0	0.06
66	−0.11	0.16	0.11	0.20	11	0.11	0	−0.20
76	−3.50	4.94	1.84	2.82	99	0.43	3	−1.22
Glu								
28	0.99	−1.40	−0.16	−1.07	47	0.15	1	0.33
31	0.38	−0.54	−0.21	−1.10	15	0.07	0	0.44
46	−0.82	1.16	0.73	−1.24	52	0.23	1	0.33
58	−0.47	0.66	1.66	2.14	83	0.44	2	0.07
82	−1.16	1.64	1.87	2.24	73	0.21	2	−0.46
102	0.76	−1.07	−1.30	−0.81	32	0.21	0	−0.27
His								
27	0.78	1.10	2.09	1.64	71	0.25	1	−0.07
40	1.45	2.04	2.04	1.12	78	0.30	2	−0.26
92	1.01	1.42	1.73	1.14	83	0.36	1	−0.40

[a] $\Delta pK = pK$ (measured) − pK (uncharged peptide). The pK values are given in Table 1.
[b] $\Delta G = 2.303RT(\Delta pK) = \gamma 1.36(\Delta pK)$ (γ is −1 for acidic groups and +1 for basic groups.
[c] The energy calculated by Coulomb's Law with $\varepsilon = 45$ for placing a charge of ±0.5 on the ionizable group at pH = pK. See the text for details.
[d] The energy calculated by UHBD with $\varepsilon = 45$ for charge–charge interactions between the ionizable group and all of the other charges on the protein.
[e] The average % buried calculated by the Lee and Richards [41] procedure for: Oδ1 and Oδ2 of the Asp residues; Oε1and Oε2 of the Glu residues; and Nδ1 and Nε2 of the His residues.
[f] The Born energy term calculated by UHBD.
[g] The number of intramolecular hydrogen bonds formed by the ionizable side chain determined using the program pfis 3.0 [42].
[h] This background energy term calculated by UHBD sums the interaction between the charge on the ionizable group and the partial charges of the polar groups in the protein.

groups are raised and some are lowered, but all of the histidine pK values are raised. This is consistent with the net charge of the protein influencing the pK values since the pI of RNase T1 is ≈4 [22]. In the next column, we convert the ΔpK term to a free energy term, denoted ΔG, using the equation given in Table 2. The other ΔG terms in Table 2 are also given in terms of free energy.

3.1. Coulomb's Law

The ΔG_{ij}(CL) term gives the energy required to place a charge of ±0.5 on the ionizable group being considered at a pH = pK of the ionizable group. In every case but one, when the ΔG_{ij}(CL) term is favorable, the pK is lowered and when it is unfavorable, the pK is raised. (The outlier is Asp 29, which will be discussed below.) This is illustrated by the ΔpK and ΔG_{ij}(CL) values in Table 2 and is a reflection of the fact that charge–charge interactions play the dominant role in determining the pK values of most ionizable groups.

The ΔG_{ij}(CL) term takes into account the actual charge on each group and its distance from the ionizing group being considered. We can also look at the relationship between the pK (measured) values and the net charge on the protein which can be calculated from the pK (measured) values. The net charge of RNase T1 is plotted as a function of pH in Fig. 2a. Note that net charge depends sharply on pH near the pI ≈ 4 of RNase T1 where the carboxyl pK values are measured. In Fig. 2b,

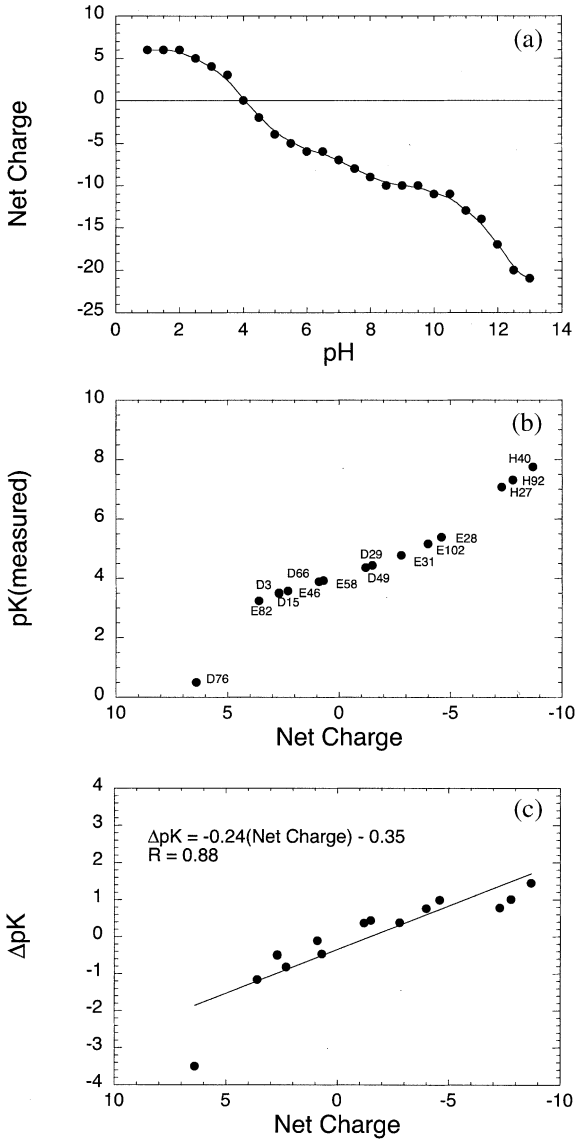

Fig. 2. Shown are plots of the net charge of RNase T1 as a function of pH (a), pK (measured) as a function of the net charge of RNase T1 (b), and $\Delta pK = pK$ (measured) $- pK$ (model compound) as a function of the net charge of RNase T1 (c). The net charge was calculated from the measured pK values in Table 1 and the model compound pK values from Nozaki and Tanford [17] for the pKs not measured. If the data point for Asp 76 is removed, $\Delta pK = -0.18$(net charge)–0.13 with $R = 0.95$.

the measured pK values are plotted as a function of the net charge, which ranges from +7 at the pK of Asp 76 to −8 near the pK values of the histidines. In Fig. 2c, the difference between the measured pK values and the pK values of model compounds is plotted as a function of the net charge. This again shows the importance of the net charge on the protein in determining the pK values. Since the net charge on a protein can be determined from a potentiometic titration curve, [23] it might be possible to estimate some of the pK values of the ionizable groups of the protein once the net charge is known as a function of pH. The discussion below will show when this approach is most likely to fail.

We have used $\varepsilon = 45$ in calculating the pK (CL) values. This is intermediate between the value for water at 35 °C, $\varepsilon = 75$, and the values commonly assumed for proteins, $\varepsilon = 2$–4 [24]. As often pointed out by the Warshel group, it is unrealistic to try and model the interior of a protein with a single dielectric constant [15]. They have also shown that the dielectric constant that is optimal for the Born self-energies is not optimal for charge–charge interactions [15]. However, using CL and $\varepsilon = 45$, 10 of the 15 pK values are predicted to better than 0.5 pK units. (Those pK values that differ by more than 0.5 pK units will each be discussed below.) If we calculate the pK (CL) values with $\varepsilon = 75$, the fit equivalent to Fig. 1a becomes $y = -1.10 + 1.22x$ with $R = 0.91$ and RMSD = 0.82. If we calculate the pK (CL) values with $\varepsilon = 20$, the fit becomes $y = 1.79 + 0.60x$ with $R = 0.92$ and RMSD = 1.31. Thus, the fit with $\varepsilon = 45$ is substantially better indicating that the average ε modulating the electrostatic interactions among the ionizing groups is intermediate between the $\varepsilon_{protein}$ and $\varepsilon_{solvent}$ values, and this seems reasonable.

Note that the pK values of Glu 28, Asp 29 and Glu 31 are all greater than the value expected based on model compounds. Residues 13 to 29 in RNase T1 form an α-helix and the ionizable groups of Lys 25, Glu 28, Asp 29 and Glu 31 are near the C-terminal end of the helix. The pH dependence of the interactions among these groups has been studied in the intact protein by Walter et al. [25] and in the isolated peptide by Myers et al.

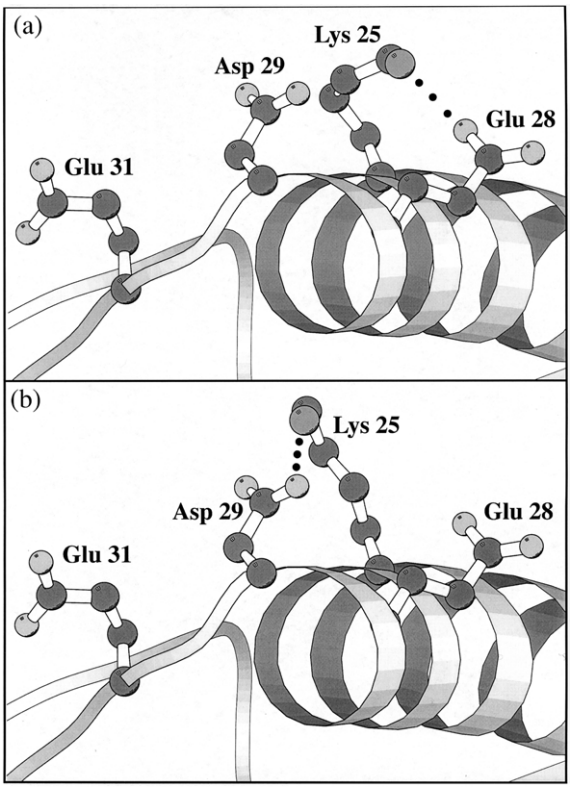

Fig. 3. MOLSCRIPT [43] ribbon diagrams illustrating the two conformations (a,b) of Lys 25 in the X-ray crystal structure 9RNT [18].

[26]. The agreement between the results for the peptide and the protein is remarkably good. Both studies show that the pK values of Glu 28 and Asp 29 are elevated in the folded protein and helical form of the peptide, suggesting this elevation of pK values results in part from an unfavorable interaction between these residues and the negative end of the helix dipole. To test this, we tried the CL calculation after adding a charge of +0.5 to the N of Ser 13 and −0.5 to the O of Asp 29 [27–31]. This improved the RMSD for all 15 ionizable groups from 0.72 to 0.68, and the pK (CL) values increased from 4.52 to 4.59 for Glu 28, from 3.57 to 3.82 for Asp 29 and from 4.55 to 4.77 for Glu 31. This shows that the helix dipole can significantly alter the pK values of ionizable groups in a protein. UHBD does better at predicting these pK values than CL which probably shows that the ΔG(BG) term in UHBD is able to capture some of the effect of the helix dipole.

Both Walter et al. [25] and Spitzner et al. [1] observed a complex titration behavior for Asp 29. The crystal structure of RNase T1 was determined at pH 7 [18]. In the crystal at pH 7, the side chain of Lys 25 is found in two conformations A and B, approximately equally populated. In A, the ζN of the Lys forms a salt bridge with Glu 28 and in B it forms a salt bridge with Asp 29 (Fig. 3). The NMR structure suggests that the side chain of Lys 25 is flexible and adopts a number of conformations. Thus, it seems likely that as the pH is lowered these groups will rearrange to give the most favorable electrostatic interactions, and this makes it difficult to predict the pK values. The importance of rearrangements of the structure during titration has been emphasized by the Warshel group [15] and is probably the reason that it is difficult to predict pK values in a case like this where there are several ionizable groups in close proximity.

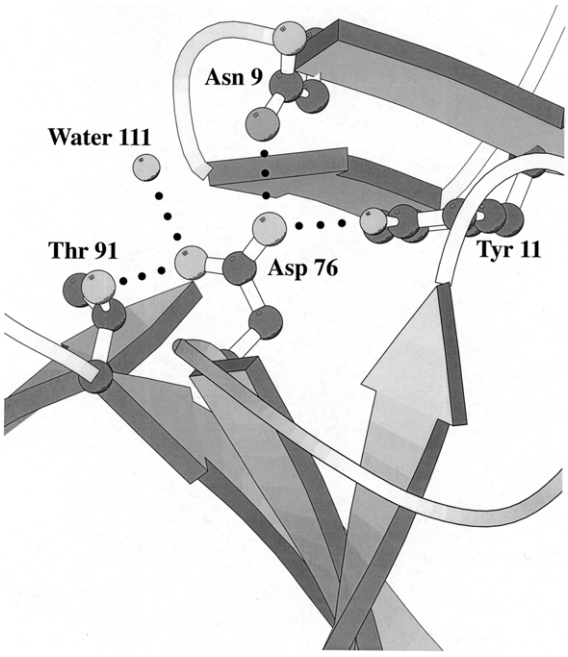

Fig. 4. MOLSCRIPT [43] ribbon diagram showing the hydrogen-bonding network of Asp 76 in RNase T1.

3.2. UHBD

In addition to the charge–charge interaction term, UHBD takes into account the Born self energy, ΔG(Born). The Born term is always positive because burying a charge is unfavorable. It will raise the pK values of carboxyl groups and lower the pK values of amino groups since the uncharged form is favored. The most buried ionizable residue is Asp 76 with ΔG(Born) = 0.43 and the most exposed is Asp 49 with ΔG(Born) = 0.05. If the percent buried is plotted as a function of ΔG(Born), the correlation coefficient is 0.90, as expected.

Both CL and UHBD predict a pK for Glu 58 that is much too low. The Born and charge–charge interaction terms for Glu 58 are large. ΔG(Born) = 0.44, and based on this value, a high pK would be expected. However, ΔG_{ij}(UHBD) = 2.14 kcal/mol, which more than overcomes the ΔG(Born) term and leads to a very low predicted pK. In contrast, CL predicts that the charge–charge interaction term to be 1.66 kcal/mol. This value is smaller than the charge–charge term for UHBD, and since there is no Born term, the predicted pK is in better agreement with experiment. Glu 58 is at the active site of RNase T1 and forms a salt bridge with His 40. It is also quite close to the positive charges of His 92 and Arg 77. Thus, at its pK Glu 58 experiences a greater positive charge than all of the carboxyl groups except Asp 76 and Glu 82, although its pK is considerably higher. The NMR structures [19] suggest that this region of the molecule is also quite flexible. It seems likely that the structure will change as the pH is lowered and the groups titrate, so the structure near Glu 58 may be quite different at pH = pK = 3.93 than it is at pH 7. This is probably the reason that both CL and UHBD substantially underestimate the pK of Glu 58. McNutt et al. [32] have shown that the pK values of all three His residues in RNase T1 are lowered in a mutant where Glu 58 is replaced by Ala, confirming the importance of charge–charge interactions in determining the pK values of these groups.

UHBD also takes into account the interactions between the ionizing group and the partial charges of the polar groups in the protein, ΔG(BG). When ΔG(BG) is negative, it will generally lower the pK values of carboxyl groups and raise the pK values of amino groups. The only ionizable group that forms three good intra-molecular hydrogen bonds (2.63, 2.69 and 2.89 Å in length) and one good intermolecular hydrogen bond to Water 111 (2.66 Å) is Asp 76 (Fig. 4), and it has the most negative value of ΔG(BG). Based on studies of the pH dependence of the stability of the wild type protein and the D76N mutant, this group has a pK = 0.5 in the folded protein and a pK = 3.7 in the unfolded protein [33]. This is remarkable since the side chain of Asp 76 is 99% buried and the distance to the nearest positive charges is 6.4 Å to Arg 77 and 8.5 Å to His 92. We think this is a good illustration of the suggestion of Warshel that often times ionizable groups can be solvated better in the interior of a protein than they can be hydrated by water [15].

Spitzner [1] and Koumanov [2] at first suggested that Asp 76 might have a high pK of approximately 6.5, but in a later paper they revised this down to a p$K \approx 2$ [3]. The pK of Asp 76 is 3.5 pK units lower than expected based on model compounds (Table 1). The best calculated value in Table 1 is pK (combined) = 2.13, which is 1.63 pK units too high. However, none of these calculations take into account Water 111 which forms a good (2.66 Å) hydrogen bond to Asp 76 and has the lowest B factor of any water in the RNase T1 crystal structure [18,34,35]. If we include Water 111 in the UHBD calculations (TIP3P parameters for water) [36], the ΔG(BG) term decreases from −1.22 to −1.62 and this lowers the predicted pK (UHBD) from 2.56 to 1.24. When these values are used in the calculations to give pK (combined), the pK = 1.86 for Asp 76, and the RMSD for all 15 ionizable groups is lowered to 0.48. These results illustrate convincingly that intramolecular hydrogen bonds with other polar groups and intermolecular hydrogen bonds to water molecules can substantially lower the pK values of carboxyl groups in proteins. Several carboxyls have been shown to have pK values <2 in other proteins [37–40] but in most cases they are involved in salt bridges. Asp 76 in RNase T1 shows that buried carboxyl groups in proteins can have very

low pK values even when they do not form salt bridges.

Note that all three of the histidine residues in RNase T1 have substantially elevated pK values (Table 1). This is in contrast to the basic protein staphylococcal nuclease (pI > 10) where all four of His residues have depressed pK values ranging from 5.30 to 6.52 in the wild type protein [16]. The results in Table 2 show clearly why the pK values are elevated in RNase T1. Both the CL and UHBD calculations show that positive charges on His side chains have favorable interactions with the other charges on the protein, and this will increase their pK values. In addition, all three of His residues are hydrogen bonded, and this will also increase the pK values. In contrast, the three His side chains are all substantially buried and this would lower their pK values. In this case, the ΔG_{ij}(UHBD) and ΔG(BG) terms outweigh the ΔG(Born) term and this leads to the elevated pK values.

3.3. Concluding remarks

In the microbial ribonuclease family, the pK values of the carboxyl groups range from 0.5 (Asp 76 in RNase T1) [33] to 7.4 (Asp 79 in RNase Sa) (Pace et al., unpublished results). The large difference between the values for the two Asp residues is especially interesting because both of the groups are almost completely buried. (Incidentally, when Val 66 in the hydrophobic core of staph nuclease is replaced with a Glu, the p$K \approx 8.8$ [12]. This value appears to be the highest pK observed for a carboxyl group in a protein.) The high pK of Asp 79 in RNase Sa results because the unfavorable ΔG(Born) term is not compensated by favorable intramolecular hydrogen-bonding or charge–charge interactions. At the other extreme, the pK of Asp 76 in RNase T1 is low because the unfavorable ΔG(Born) term can be more than overcome by favorable hydrogen bonding and longer-range charge–charge interactions. The results in Table 2 show that in UHBD, the ΔG_{ij}(UHBD) term is generally larger than the ΔG(Born) and ΔG(BG) terms, especially when the pH being considered is not near the pI of the protein.

Acknowledgments

This research was supported by the National Institutes of Health (GM37039 and GM52483) and the Robert A. Welch Foundation (BE-1060 and BE-1281). CNP is supported by the Tom and Jean McMullin Professorship and JMS is an American Heart Association Established Investigator.

References

[1] N. Spitzner, F. Löhr, S. Pfeiffer, A. Koumanov, A. Karshikoff, H. Rüterjans, Ionization properties of titratable groups in ribonuclease T1 I. pKa values in the native state determined by two-dimensional heteronuclear NMR spectroscopy, Eur. Biophys. J. 30 (2001) 186–197.

[2] A. Koumanov, N. Spitzner, H. Rüterjans, A. Karshikoff, Ionization properties of titratable groups in ribonuclease T1 II. Electrostatic analysis, Eur. Biophys. J. 30 (2001) 198–206.

[3] A. Koumanov, H. Rüterjans, A. Karshikoff, Continuum electrostatic analysis of irregular ionization and proton allocation in proteins, Proteins 46 (2002) 85–96.

[4] M.E. Davis, J.D. Madura, B.A. Luty, J.A. McCammon, Electrostatics and diffusion of molecules in solution: simulations with the University of Houston Brownian Dynamics program, Comp. Phys. Chem. 62 (1991) 187–197.

[5] J. Antosiewcz, J.M. Briggs, A.H. Elcock, M.K. Gilson, M.J. Andrew, Computing ionization states of proteins with a detailed charge model, J. Comp. Chem. 17 (1996) 1633–1644.

[6] J. Antosiewicz, J.A. McCammon, M.K. Gilson, The determinants of pKas in proteins, Biochemistry 35 (1996) 7819–7833.

[7] D. Bashford, M. Karplus, pKa's of ionizable groups in proteins: Atomic detail from a continuum electrostatic model, Biochemistry 29 (1990) 10219–10225.

[8] A.S. Yang, M.R. Gunner, R. Sampogna, K. Sharp, B. Honig, On the calculation of pKas in proteins, Proteins 15 (1993) 252–265.

[9] E.L. Mehler, F. Guarnieri, A self-consistent, microenvironment modulated screened coulomb potential approximation to calculate pH-dependent electrostatic effects in proteins, Biophys. J. 77 (1999) 3–22.

[10] J.E. Nielsen, K.V. Andersen, B. Honig, et al., Improving macromolecular electrostatics calculations, Protein Eng. 12 (1999) 657–662.

[11] G.M. Ullmann, E.-W. Knapp, Electrostatic models for computing protonation and redox equilibria in proteins, Eur. Biophys. J. 28 (1999) 533–551.

[12] J.J. Dwyer, A.G. Gittis, D.A. Karp, et al., High apparent dielectric constants in the interior of a protein reflect water penetration, Biophys. J. 79 (2000) 1610–1620.

[13] W.R. Forsyth, A.D. Robertson, Insensitivity of perturbed carboxyl p*K*(a) values in the ovomucoid third domain to charge replacement at a neighboring residue, Biochemistry 39 (2000) 8067–8072.
[14] J.W. Pitera, M. Falta, W.F. van Gunsteren, Dielectric properties of proteins from simulation: The effects of solvent, ligands, pH and temperature, Biophys. J. 80 (2001) 2546–2555.
[15] C.N. Schutz, A. Warshel, What are the dielectric 'constants' of proteins and how to validate electrostatic models?, Proteins 44 (2001) 400–417.
[16] B.K. Lee, C.A. Fitch, B. Garía-Moreno E., Distance dependence and salt sensitivity of pairwise, coulombic interactions in a protein, Protein Sci. (2002) in press.
[17] Y. Nozaki, C. Tanford, Examination of titration behavior, Methods Enzymol. 11 (1967) 715–734.
[18] J. Martinez-Oyanedel, U. Heineman, W. Saenger, Ribonuclease T1 with free recognition and catalytic site: crystal structure analysis at 1.5A resolution, J. Mol. Biol. 222 (1991) 335–352.
[19] S. Pfeiffer, Y. Karimi-Nejad, H. Ruterjans, Limits of NMR structure determination using variable target function calculations: ribonuclease T1, a case study, J. Mol. Biol. 266 (1997) 400–423.
[20] E. Neria, S. Fischer, M. Karplus, Simulation of activation free energies in molecular systems, J. Chem. Phys. 105 (1996) 1902–1921.
[21] A.-S. Yang, B. Honig, On the pH dependence of protein stability, J. Mol. Biol. 231 (1993) 459–474.
[22] E.J. Hebert, G.R. Grimsley, R.W. Hartley, et al., Purification of ribonuclease Sa, Sa2 and Sa3 after expression in *Escherichia coli*, Protein Exp. Purif. 11 (1997) 162–168.
[23] C. Tanford, The interpretation of hydrogen ion titration curves of proteins, Adv. Protein Chem. 17 (1962) 69–165.
[24] M.K. Gilson, B.H. Honig, The dielectric constant of a folded protein, Biopolymers 25 (1986) 2097–2119.
[25] S. Walter, B. Hubner, U. Hahn, F.X. Schmid, Destabilization of a protein helix by electrostatic interactions, J. Mol. Biol. 252 (1995) 133–143.
[26] J.K. Myers, J.S. Smith, C.N. Pace, J.M. Scholtz, The α-helix of ribonuclease T1 as an independent stability unit: Direct comparison of peptide and protein stability, J. Mol. Biol. 263 (1996) 390–395.
[27] A. Wada, The α-helix as an electric macro-dipole, Adv. Biophys. 9 (1976) 1–63.
[28] W.G.J. Hol, P.T. van Duijnen, H.J.C. Berendsen, The α-helix dipole and properties of proteins, Nature 273 (1978) 443–446.
[29] R.P. Sheridan, R.M. Levy, F.R. Salemme, α-Helix dipole model and electrostatic stabilization of 4-α-helical protein, Proc. Natl. Acad. Sci. USA 79 (1982) 4545–4549.
[30] J.M. Scholtz, H. Qian, V.H. Robbins, R.L. Baldwin, The energetics of ion-pair and hydrogen-bonding interactions in a helical peptide, Biochemistry 32 (1993) 9668–9676.
[31] B.M.P. Huyghues-Despointes, J.M. Scholtz, R.L. Baldwin, The effect of a single aspartate on helix stability at different positions in a neutral alanine-based peptide, Protein Sci. 2 (1993) 1604–1611.
[32] M. McNutt, L.S. Mullins, F.M. Raushel, C.N. Pace, Contribution of histidine residues to the conformational stability of ribonuclease T1 and mutant Glu-58 to Ala, Biochemistry 29 (1990) 7572–7576.
[33] A. Giletto, C.N. Pace, Buried, charged, non-ion-paired aspartic acid 76 contributes favorably to the conformational stability of ribonuclease T1, Biochemistry 38 (1999) 13379–13384.
[34] S. Pfeiffer, N. Spitzner, F. Lohr, H. Ruterjans, Hydration water molecules of nucleotide-free RNase T1 studied by NMR spectroscopy in solution, J. Biomol. NMR 11 (1998) 1–15.
[35] U. Langhorst, R. Loris, V. Denisov, et al., Dissection of the structural and functional role of a conserved hydration site in RNase T1, Protein Sci. 8 (1999) 722–730.
[36] W.L. Jorgensen, J. Tirado-Rives, The OPLS potential functions for proteins. Energy minimizations for crystals of cyclic peptides and crambin, J. Am. Chem. Soc. 110 (1988) 1657–1666.
[37] M.D. Joshi, A. Hedberg, L.P. McIntosh, Complete measurement of the pKa values of the carboxyl and imidazole groups in *Bacillus circulans* xylanase, Protein Sci. 6 (1997) 2667–2670.
[38] M. Oliveberg, V.L. Arcus, A.R. Fersht, pK_A values of carboxyl groups in the native and denatured states of barnase: the pK_A values of the denatured state are on average 0.4 units lower than those of model compounds, Biochemistry 34 (1995) 9424–9433.
[39] D.E. Anderson, J. Lu, L. McIntosh, F.W. Dahlquist, NMR of Proteins, In: Clore, G.M. and Gronenborn A.M. (Eds.). The Folding, Stability and Dynamics of T4 Lysozyme: A Perspective Using Nuclear Magnetic Resonance (1993) pp. 259–303.
[40] D.E. Anderson, W.J. Becktel, F.W. Dahlquist, pH-induced denaturation of proteins: a single salt bridge contributes 3–5 kcal/mol to the free energy of folding of T4 lysozyme, Biochemistry 29 (1990) 2403–2408.
[41] B. Lee, F.M. Richards, The interpretation of protein structures: estimation of static accessibility, J. Mol. Biol. 55 (1971) 379–400.
[42] E.J. Hebert, A. Giletto, J. Sevcik, et al., Contribution of a conserved asparagine to the conformational stability of ribonucleases Sa, Ba and T1, Biochemistry 37 (1998) 16192–16200.
[43] P.J. Kraulis, MOLSCRIPT: a program to produce both detailed and schematic plots of protein structures, J. Appl. Crystallogr. 24 (1991) 946–950.